THE JOURNAL OF BIOLOGICAL CHEMISTRY VOL. 291, NO. 36, pp. 18730–18739, September 2, 2016

Fibulin-1 Binds to Fibroblast Growth Factor 8 with High Affinity

EFFECTS ON EMBRYO SURVIVAL[*]

Received for publication, November 9, 2015, and in revised form, June 29, 2016 Published, JBC Papers in Press, July 8, 2016, DOI 10.1074/jbc.M115.702761

Victor M. Fresco[‡1], **Christine B. Kern**[‡2], **Moosa Mohammadi**[§3], **and Waleed O. Twal**[‡4]

From the [‡]*Department of Regenerative Medicine and Cell Biology, Medical University of South Carolina, Charleston, South Carolina 29425 and the* [§]*Department of Biochemistry and Molecular Pharmacology, New York University School of Medicine, New York, New York 10016*

Fibulin-1 (FBLN1) is a member of a growing family of extracellular matrix glycoproteins that includes eight members and is involved in cellular functions such as adhesion, migration, and differentiation. FBLN1 has also been implicated in embryonic heart and valve development and in the formation of neural crest-derived structures, including aortic arch, thymus, and cranial nerves. Fibroblast growth factor 8 (FGF8) is a member of a large family of growth factors, and its functions include neural crest cell (NCC) maintenance, specifically NCC migration as well as patterning of structures formed from NCC such as outflow tract and cranial nerves. In this report, we sought to investigate whether FBLN1 and FGF8 have cooperative roles *in vivo* given their influence on the development of the same NCC-derived structures. Surface plasmon resonance binding data showed that FBLN1 binds tightly to FGF8 and prevents its enzymatic degradation by ADAM17. Moreover, overexpression of *FBLN1* up-regulates *FGF8* gene expression, and down-regulation of *FBLN1* by siRNA inhibits *FGF8* expression. The generation of a double mutant *Fbln1* and *Fgf8* mice (*Fbln1*$^{-/-}$ and *Fgf8*$^{-/-}$) showed that haplo-insufficiency (*Fbln1*$^{+/-}$ and *Fgf8*$^{+/-}$) resulted in increased embryonic mortality compared with single heterozygote crosses. The mortality of the FGF8/Fbln1 double heterozygote embryos occurred between 14.5 and 16.5 days post-coitus. In conclusion, FBLN1/FGF8 interaction plays a role in survival of vertebrate embryos, and reduced levels of both proteins resulted in added mortality *in utero*. The FBLN1/FGF8 interaction may also be involved in the survival of neural crest cell population during development.

Fibulin-1 (FBLN1)[5] is a member of a growing family of proteins that includes eight members (1, 2). FBLN1 binds to itself and many extracellular matrix molecules such as fibronectin (FN), nidogen, laminin, and versican (2, 3). FBLN1 has also been reported to regulate adhesion and migration of cells (4). During vertebrate development, FBLN1 is expressed along the paths of migrating neural crest cells (NCC) and by migrating endocardial cushion mesenchymal cells, suggesting that it might be a regulator of cell migrations essential to heart and pharyngeal arch morphogenesis (5–7). FBLN1 has also been shown to suppress the migratory behavior of embryonic mesenchymal cells as well as the motility and directional movement of cancer cells (4, 8, 9). Morphological analysis of FBLN1-deficient embryos showed cardiac abnormalities, which includes a high incidence of double outlet right ventricle and over-riding aorta (7). The spectrum of malformations seen in FBLN1 null mice is consistent with FBLN1 influencing NCC-dependent development of these tissues (7).

Androgen-induced growth factor was identified as the eighth member of the fibroblast growth factor (FGF8) family and is detected only in the testis of adult tissues (10). During development, expression of FGF8 is restricted to embryonic days 9–13 suggesting that the growth factor plays a role during a specific stage of mouse embryogenesis (10, 11). *FGF8a* and *FGF8b*, two variants of *FGF8* transcript, are expressed in the mid-hindbrain region during development (12). Although the only difference between FGF8a and FGF8b isoforms is the presence of an additional 11 amino acids at the N terminus of FGF8b, these isoforms possess remarkably different abilities to pattern the midbrain and anterior hindbrain (12). To reveal the structural basis by which alternative splicing modulates the organizing activity of FGF8, the crystal structure of FGF8b in complex with the "c" splice isoform of FGF receptor 2 (FGFR2c) was resolved (12).

Neural crest cells are a transient, multipotent, and migratory cell population unique to vertebrates that gives rise to diverse cell lineages, including craniofacial cartilage and bone, smooth muscle, and peripheral and enteric neurons (13). Abnormalities in neural crest development cause conditions such as frontonasal dysplasia, Waardenburg-Shah syndrome, and DiGeorge syndrome (13). FGF8 signaling has been shown to be required for neural crest delamination and migration (14). In the hindbrain, *FGF8* deficiency negatively impacts patterning of cranial nerves derived from NCCs (15). FGF8 has also been shown to regulate migration of NCCs as they travel to the caudal pharyngeal arches (14, 16, 17). Neural crest ablation results in overproliferation of secondary heart field cells due to excessive FGF8

[*] This work was supported in part by National Institutes of Health Grants R01 HL09506 and P01 HL52813 from NHLBI and Grant P30 GM103342 from NIGMS (to South Carolina COBRE for Developmentally Based Cardiovascular Diseases). The authors declare that they have no conflicts of interest with the contents of this article. The content is solely the responsibility of the authors and does not necessarily represent the official views of the National Institutes of Health.

[1] Submitted in partial fulfillment of the requirements for a Ph.D. degree at Medical University of South Carolina.

[2] Supported by National Institutes of Health Grant HL121382.

[3] Supported by NIDCR Grant R01 DE-13686.

[4] To whom correspondence should be addressed: Dept. of Regenerative Medicine and Cell Biology, Medical University of South Carolina, 173 Ashley Ave., MSC 508, Charleston, SC 29425. Tel.: 843-792-7054; Fax: 843-792-0664; E-mail: twalwo@musc.edu.

[5] The abbreviations used are: FBLN1, fibulin 1; r, recombinant; NCC, neural crest cells; qPCR, quantitative real time PCR; FN, fibronectin; dpc, days post-coitus.

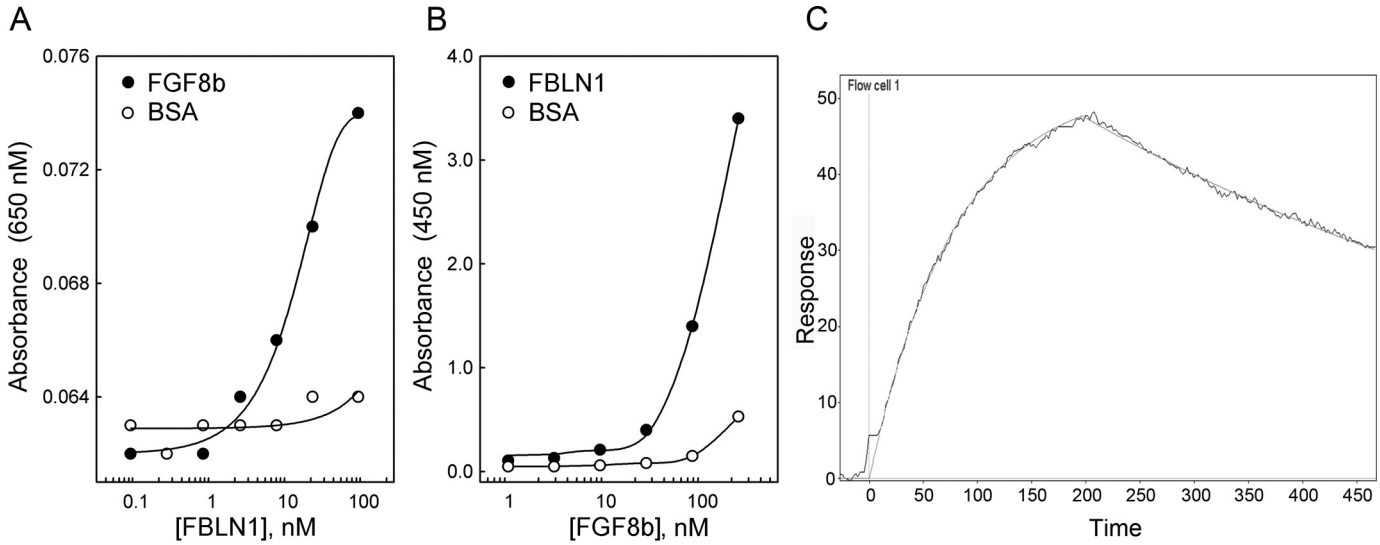

FIGURE 1. **FBLN1 binds to FGF8 with high affinity.** *A,* FBLN1 binds to FGF8b coating in a solid-phase binding assay. *B,* FGF8b binds to fibulin-1 coating in a solid-phase binding assay. Fibulin-1 was detected using Rb2954 polyclonal antibody, and FGF8b was detected using monoclonal antibody. Color development was achieved using ultra-3,3,5,5-tetramethylbenzidine detection reagent. Data are presented as mean ± range of duplicate samples and a representative of three independent experiments. *C,* binding of immobilized FGF8b to FBLN1 in a surface plasmon resonance assay using a Reichert SPR instrument.

signaling in the caudal pharynx (18) and elevated expression of FGF8 target genes *Erm* and *Pea3* (19, 20). Inhibition of FGF8 signaling following NCC ablation reversed this phenotype. Studies show that inhibition of FGF8 signaling in the absence of NCC ablation causes under-proliferation of secondary heart field cells, resulting in a shortened outflow tract (18). Additionally, it has been shown that FGF8 acts as a chemotactic and chemokinetic signal for cardiac neural crest cells both *in vitro* and *in vivo* (21). Thus, precise levels of FGF8 signaling seem critical for normal outflow tract development and morphogenesis.

Given the similarity of effects of both FBLN1 and FGF8 on NCC migration, this study investigated whether there is a collaborative role during the development of vertebrate embryos. Herein, we report the finding that FBLN1 binds to FGF8 with high affinity and protects it from enzymatic degradation. We also show that FBLN1 and FGF8 double mutant heterozygote embryos show a synergistic effect on mortality compared with either FGF8 or FBLN1 null heterozygote embryos alone.

Results

Binding of FBLN1 to FGF8—We employed an ELISA procedure to test whether FBLN1 binds to FGF8. When plates were coated with FGF8b, and FBLN1 was added in solution phase, the apparent affinity constant (K_D) of the interaction was about 20 nM (Fig. 1*A*). When FBLN1 was coated on the surface and FGF8b was in solution phase, the apparent K_D was about 100 nM but was not saturable due to the propensity of FBLN1 to bind to itself (Fig. 1*B*). When the surface plasmon resonance technique was used, the association constant (K_a) was $3.47 \times 10^4\ \mathrm{M}^{-1}\ \mathrm{s}^{-1}$; the dissociation constant (K_d) was $1.71 \times 10^{-3}\ \mathrm{s}^{-1}$, and the affinity constant (K_D) was about 50 nM (Fig. 1*C*).

FBLN1 Protects FGF8b from Enzymatic Degradation—We tested whether FBLN1 binding to FGF8b protects it from enzymatic degradation catalyzed by a disintegrin and metallopeptidase domain 17/tumor necrosis α convertase (ADAM17/TACE). When FBLN1 was co-incubated with FGF8b and ADAM17, little degradation of FGF8b occurred (Fig. 2*A*, *lane 4*), whereas ADAM17 alone caused complete degradation of the FGF8b (Fig. 2*A*, *lane 3*). Addition of EDTA to FGF8b prevented the apparent slight degradation (Fig. 2*A*, *lane 5*) that was seen when FGF8b was incubated without added enzyme or FBLN1 for 18 h (Fig. 2*A*, *lane 1*). In Fig. 2*A*, *lane 6*, FGF8 was not incubated for 18 h. Re-blotting the membrane with anti-ADAM17/TACE antibodies showed the presence of the enzyme in *lanes 3* and 4 at a molecular mass of about 52 kDa, which represents the ectodomain portion of ADAM17 (Fig. 2*B*).

FLBN1 Inhibits Activation of FGF8b Signaling—We tested the ability of FBLN1 to modulate FGF8b signaling. When FGF8b was bound to FBLN1 before addition to NIH 3T3 cells, the phosphorylation of ERK1/2 induced by the addition of FGF8b alone was greatly reduced using immunoblot analysis (Fig. 3*A*, *upper panel*). Addition of FBLN1 to FGF2 did not have any effect on the phosphorylation of ERK1/2 (Fig. 3*B*, *upper panel*). We then employed a Luminex-based multiplex assay to quantitate the extent of the inhibition of ERK1/2 phosphorylation by FBLN1, rFBLN1C, and rFBLN1D (Fig. 3*C*), and we found that both FLBN1 variants C and D as well as FBLN1 reduced the ERK1/2 phosphorylation signal by about 50%.

Purified Preparations of Fibulin-1 Contain Bound FGF8—We tested whether preparations of FBLN1 have a detectable activity of FGF8. As shown in Fig. 4*A* (*left panel*), detection of FBLN1 preparations with anti-FGF8 monoclonal antibody revealed the presence of two high molecular mass bands at about 120 and 175 kDa (Fig. 4*A*, *arrows*). When preparations were re-probed with monoclonal and polyclonal antibodies against FBLN1 (Fig. 4*A*, *middle* and *right panel*), both monomeric and dimeric FBLN1 forms were detected. The high molecular weight complexes detected in Fig. 4*A* (*left panel*) were also detected in rFBLN1C or rFBLN1D preparations, purified from HT1080 *FBLN1C* or *FBLN1D*-transfected cells,

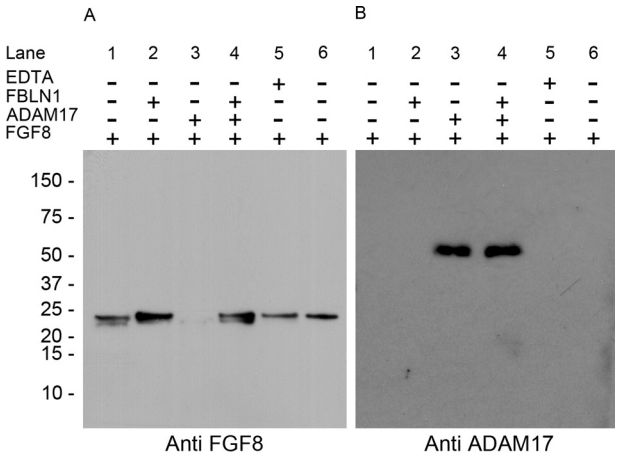

FIGURE 2. **Placental fibulin-1 protects FGF8b from enzymatic degradation.** FGF8b (150 ng) was incubated with and without ADAM17 (0.2 μg) in the presence or absence of FBLN1 (1.4 μg). After 18 h of incubation, 10 μl of 4× sample buffer was added to the 30-μl reaction mixture and then loaded on 4–12% NUPAGE gel. Proteins were then transferred to a PVDF membrane. FGF8 was detected using monoclonal primary antibodies and anti-mouse horseradish peroxidase (HRP)-conjugated IgG. Visualization was done using ECL chemiluminescent reagent (*A*). Reblotting with ADAM17/TACE antibodies detected the enzyme *lanes 3* and *4* (*B*). Data presented are representative of three independent experiments.

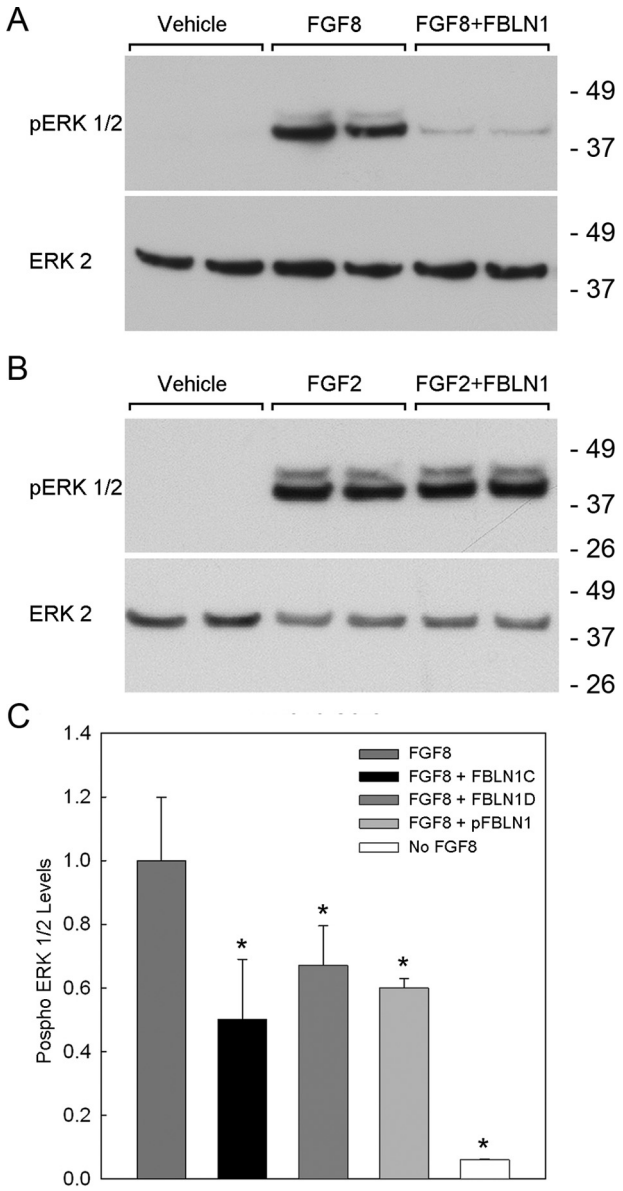

FIGURE 3. **Fibulin-1 inhibits activation of FGF8 phosphorylation of ERK1/2.** *A,* NIH 3T3 cells were incubated with FGF8b (24 ng/ml) in the presence or absence of FBLN1 (2 μg). *B,* FGF2 was used as a control protein in *A*. Immunoblot analysis of ERK1/2 was performed using monoclonal antibodies, anti-mouse secondary antibodies, and ECL chemiluminescent reagent. *C,* in a parallel experiment pERK1/2 was quantified by Luminex-based assay using a Bioplex 200 instrument after treatment of NIH 3T3 cells with FGF8b in the presence of fibulin-1C or -1D or placental fibulin-1 (*Fbln1*) as described in *A*. Data presented are representative of three independent experiments. * denotes significance from FGF8 alone, $p < 0.05$.

as shown in Fig. 4*B* (*left panel, arrows*). It is possible that FGF8 binds to monomer as well as to the dimer forms of FBLN1. Detection of FGF8 binding to rFBLN1C is much lower than that of rFBLN1D (Fig. 4*B*, *left panel, arrows*), which can be due to the masking of the FGF8 epitope by rFBLN1C binding to FGF8 but is not in the case of rFBLN1D binding to FGF8. Re-probing the blot with polyclonal antibodies against FBLN1 (Fig. 4*B*, *left panel*) detected the presence of both FBLN1 isoforms C and D. We also tested whether we were able to immunoprecipitate FGF8b using FBLN1-conjugated Sepharose. FBLN1-bound Sepharose immunoprecipitated FGF8b (Fig. 4*C*, *2 left lanes*), although plain Sepharose did not bind any FGF8b (*2 right lanes*). The apparent decrease in molecular mass of FGF8 when incubated with plain Sepharose is probably due to enzymatic degradation that occurred in some FGF8 preparations during the 18-h incubation.

siRNA Inhibition of FBLN1 Expression Decreases FGF8 mRNA Levels in P19.C16 Mouse Embryonic Teratocarcinoma Cells—We have chosen the mouse embryonic teratocarcinoma cell line P19.C16 to test whether levels of *Fbln1* affect *Fgf8* expression, which is transiently elevated during differentiation of the cell line. We used quantitative real time PCR (qPCR, Table 1) to detect *Fgf8*, *Fbln1C*, and *Fbln1D* mRNA expression for 5 days after transfection of the cells with *Fbln1* siRNA. Transient inhibition of *Fbln1* expression reduced *Fgf8* mRNA expression (Fig. 5, *upper panel*). Results indicate that *Fgf8* expression was decreased by about 30%, and *Fgf8* peak expression was shifted by about ½ day (2 days *versus* 2½ days, Fig. 5, *upper panel*). Expression of both *Fbln1C* and *Fbln1D* mRNA returned to the levels of control siRNA-transfected cells at day 5 (Fig. 5, *middle* and *lower panel*, respectively).

Overexpression of FBLN1C or -1D Induces the Expression of FGF8 in HT1080 Cells—Using qPCR (primers are listed in Table 1), we tested the effect of overexpression of *FBLN1C* and *FBLN1D* in stably transfected HT1080 on expression of *FGF8*. Both *FBLN1D* and *1C* increased the expression of *FGF8* by 1.7–2.7-fold, respectively, compared with empty vector-transfected cells when normalized to the amount of *FBLN1* expression of each cell line (Fig. 6).

Fgf8 and Fbln1 Co-localized in the Cardiac Outflow Tract of 10.5 dpc Mouse Embryos—Immunohistochemistry was performed to determine the *in vivo* localization of Fgf8 and Fbln1 (Fig. 7). Previous studies have demonstrated that Fgf8 and Fbln1 are present at developmental time points where cardiac neural crest and anterior heart field cells migrate to and populate the cardiac outflow tract (7, 19). Using histological sections

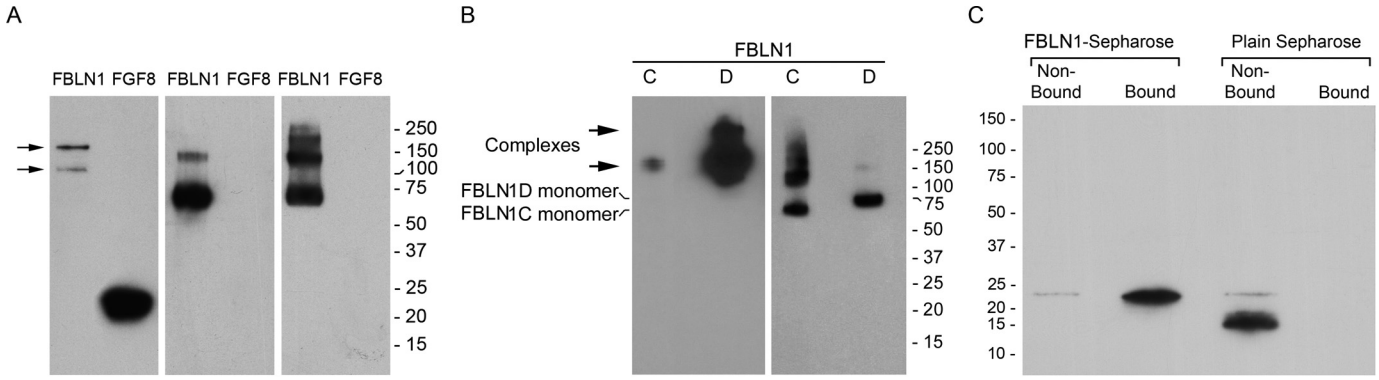

FIGURE 4. **Placental fibulin-1 (FBLN1) preparations contain FBLN1-bound FGF8.** *A,* FBLN1 has FGF8 bound to it (*arrows, left panel*). *Middle* and *right panels* show FBLN1 detection using the polyclonal anti-FBLN1 antibody (Rb2954) and the monoclonal anti-FBLN1 IgG (3A11), respectively. *B,* recombinant Fbln1C and -1D preparations also contain complexes of FBLN1 and FGF8 as detected by mAb against FGF8 (*left panel, arrows*) although re-probing with polyclonal antibody against Fbln1 detected the presence of FBLN1C and -1D monomers and dimers (*right panel*). *C,* FGF8b was incubated with FBLN1-conjugated Sepharose, and bound and unbound (*2 left lanes*) fractions were immunoblotted with anti-FGF8 monoclonal antibody. Anti-mouse HRP-conjugated antibody and ECL+ were used to detect bound and unbound fractions of FGF8. Plain Sepharose was used as a negative control (*2 right lanes*). The slight decrease of the FGF8 molecular weight was due to an enzymatic activity that was found to be present in some of the FGF8 preparations. Data presented are representative of two independent experiments.

TABLE 1
Primers used for PCR, real time PCR, and mouse genotyping

Gene	Type	Sequence	Reference sequence no.
Fibulin 1C	Forward	caactgctccatcaacgaga	NM_001996.3
	Reverse	attctcagaggcagcttgga	
Fibulin 1D	Forward	cgagtgccctgagaactacc	NM_006486.2
	Reverse	gagatgacggtgtgggagat	
Human FGF8	Forward	ggaagctgatcgccaaga	U46211.1
	Reverse	ttctgcagcgctgtgtagt	
GAPDH	Forward	atgttcgtcatgggtgtgaa	NM_001256799.1
	Reverse	ggtgctaagcagttggtggt	
TATA box BP	Forward	cggctgtttaacttcgcttc	BT019657.1
	Reverse	ctgggtcactgcaaagatca	
Fibulin 1 genotyping	Forward	agccccagctgattctgaactcctgacc	NM_010180
	Reverse	gcaacagcagtgttgggtggaggaaggg	
CD4	Forward	ctcctacatagttggcagtgtttggg	BC039137.1
Mouse FGF8 Wild-type allele	Forward	tgcctaaggggagaaggctgg	Z46883.1
	Reverse	aaatttaagctgtgtagattccatag	
Mouse FGF8 Recombinant mutant allele	Forward	tgcctaaggggagaaggctgg	Z46883.1
	Reverse	gatttcaggagaacagaccagag	

from developing mice, hearts were immunostained for Fbln1 (Fig. 7, *A* and *C* (*green*)) and Fgf8 (Fig. 7, *A* and *C* (*blue*)). IgG control sections are depicted in Fig. 7, *B* and *D*.

Genotypic Analysis of 4-Week-old Mice from Fgf8/Fbln1 (Fgf8$^{+/-}$ and Fbln1$^{+/-}$) Heterozygote Cross and Fgf8/Fbln1 Double Heterozygote Cross (Fgf8$^{+/-}$ Fbln1$^{+/-}$ Sibling Cross)—Mice heterozygous for Fgf8 were mated with mice heterozygous for Fbln1 and offspring were genotyped at 4 weeks of age. As shown in Table 2, the number of animals and the expected ratio of double Fgf8/Fbln1 heterozygotes were lower than the predicted Mendelian ratios (16% *versus* 25%), indicating increased mortality of double heterozygote animals compared with the Fgf8 or Fbln1 heterozygote cross alone. When animals that were heterozygote for Fgf8/Fbln1 were crossed with each other, the expected Mendelian ratio for the double heterozygote was also lower (33% *versus* 44%, see Table 3). When genotyping was performed on embryos at 10.5, 14.5 (Table 4), 16.5 (Table 5), and 18.5 dpc, the expected Mendelian ratio was lower at 16.5 dpc (Table 5, 20% *versus* 33%) but not at 14.5 dpc (Table 4, 33% *versus* 32%), indicating that the mortality in the double heterozygote embryos occurred between 14.5 and 16.5 dpc. All surviving embryos at 16.5 and 18.5 dpc and 4 weeks of age were examined for heart and cranial nerve developmental defects, but none were detected. The absence of any abnormalities in the surviving embryos and adult mice led us to speculate that these abnormalities might be present in the animals that die and were resorbed between 14.5 and 16.5 dpc.

Discussion

In this report, we have investigated whether FBLN1, a known extracellular glycoprotein (7) as well as an intracellular integrin β1-binding protein (22), and FGF8, a known effector of NCC migration (21), associate with each other biochemically and have synergistic effects on embryonic development or survival. Herein, we show for the first time that FBLN1 binds with high affinity to FGF8 and protects it from enzymatic degradation by ADAM17. Additionally, overexpression of *FBLN1* stimulates *FGF8* mRNA production, although siRNA inhibition of FBLN1 down-regulates *FGF8* message. Adult mice at 4 weeks of age that are heterozygote for both Fbln1 and Fgf8 show increased embryonic mortality compared with single heterozygote animals. By examining embryos at different developmental stages (10.5–18.5 dpc), it was determined that loss of double heterozygote animals *in utero* occurs between 14.5 and 16.5 dpc.

We have previously shown that Fbln1 is expressed along the paths of migrating NCCs (7) and by migrating endocardial

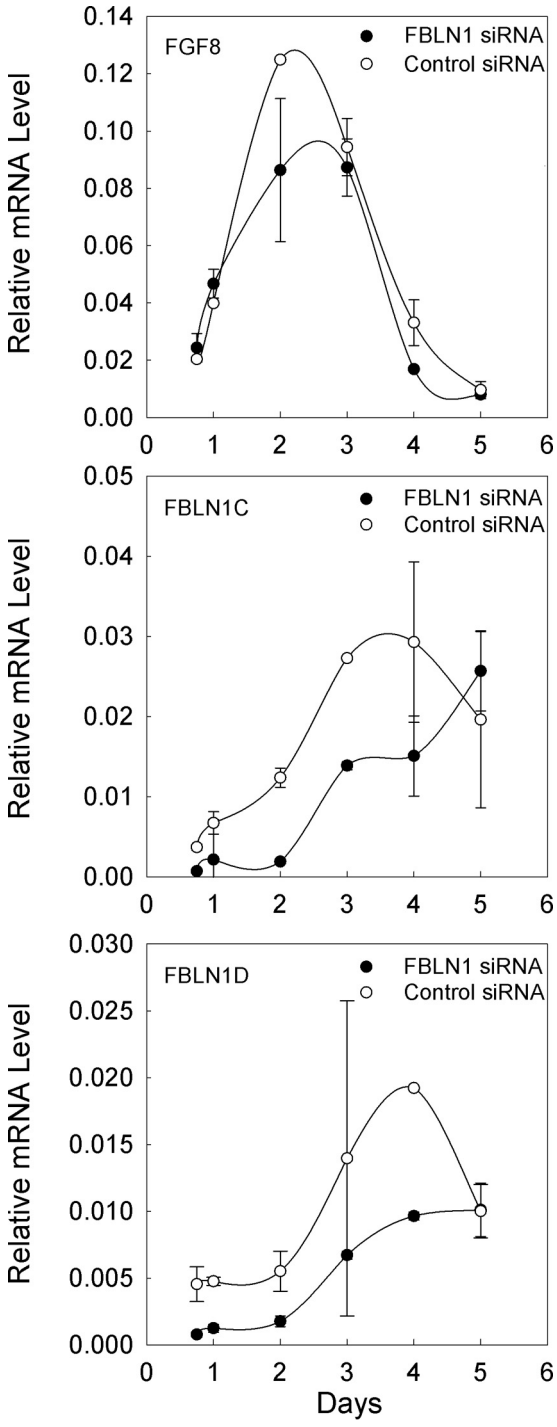

FIGURE 5. **Inhibition of fibulin-1 decreases the expression of *FGF8* expression.** P19 cells were treated with fibulin-1 siRNA for 2 days. *Upper panel* depicts inhibition of Fgf8 message expression over a period of 5 days. *Middle* and *lower panels* depict inhibition of fibulin-1C (*Fbln1C*) and fibulin-1D (*Fbln1D*), respectively. Data are presented as mean ± range of duplicate samples and as representative of three independent experiments.

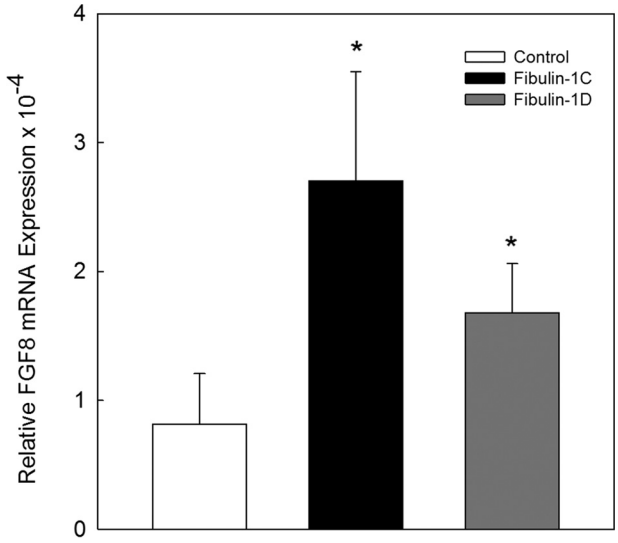

FIGURE 6. **Overexpression of FBLN1C or -1D induces the expression of *FGF8* mRNA.** HT1080 cells stably transfected with FBLN1C or -1D were cultured on FN-coated dishes, and RNA was extracted and probed for *FGF8* expression. *FGF8* expression levels were normalized to the levels of FBLN1 in each cell line. Data are presented as mean ± range of duplicate samples and as representative of two independent experiments. *Asterisk* denotes significance from control, $p < 0.05$.

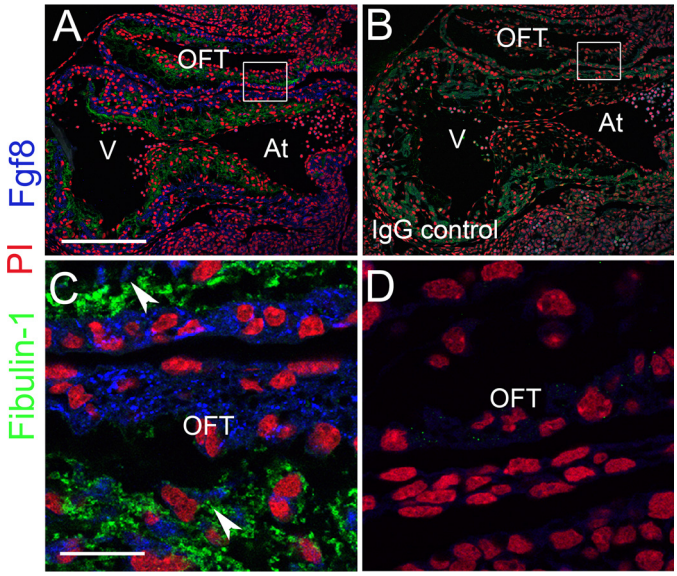

FIGURE 7. **Fgf 8 and Fbln1 colocalized in developing murine hearts.** Histological sections from 10.5 dpc murine hearts were immunolocalized with antibodies to Fgf 8 (*A* and *C, blue*) and Fbln1 (*A* and *C, green*). *B* and *D* were treated with IgG and secondary antibodies as controls. *Arrowheads* denote examples of colocalization of FGF8-Fbln1 in the cardiac outflow tract. *Red* indicates propidium iodide staining (*PI*). *V,* ventricle; *At,* atrium; *OFT,* outflow tract. *Bar* in *A,* 200 μm and also applies to *B*; *C,* 20 μm and also applies to *D*.

cushion mesenchymal cells (5, 6, 9), suggesting that it might be a regulator of cell migration essential to heart and pharyngeal arch morphogenesis. Morphological analysis of Fbln1-deficient embryos has also been shown to exhibit cardiac and outflow tract abnormalities, which include a high incidence of double outlet right ventricle and over-riding aorta (7). Fbln1-deficient embryos examined at stages 16.5–18.5 dpc also exhibit hypoplastic thymus with 100% penetrance. This observation further implicates Fbln1 importance in NCC migration due to the fact that the thymus is derived from the third pharyngeal arch (23) and is dependent on neural crest-derived mesenchymal cells.

The extracellular matrix protein FN has also been implicated in affecting migration of NCC populations (24, 25). This role has been shown to be in part through interactions with $\alpha5\beta1$ integrin. Conditional $\beta1$ integrin gene deletion in NCCs causes severe developmental alterations of the peripheral nervous sys-

TABLE 2

Genotyping of a single heterozygote cross of Fgf8 and Fbln1 mice

Mouse heterozygotes for Fgf8 were crossed with Fbln1 heterozygote mice, and animals were genotyped at 4 weeks of age. The number of animals for the double heterozygote animals was lower than the expected Mendelian ratio as indicated by the boldface number. The χ^2 statistics test was used to calculate a p value to determine significant deviation from normal expected Mendelian genotypic ratios. Animals with a $-/-$ genotype for the Fgf8 allele (boldface symbol) were embryonic lethal and were neither expected to survive nor observed and were not included in the calculation. χ^2 test was significant at $X^2 = 0.041$.

Genotype (Fgf8) (Fbln1)	% expected[a]	% observed	No. expected[a]	No. observed
(**+**/**+**) (+/+)	25%	28%	37	42
(**+**/**+**) (+/−)	25%	29%	37	43
(**+**/**−**) (+/+)	25%	37%	37	39
(**+**/**−**) (+/−)	25%	**16%**	37	24
Total	100%	100%	148	148

[a] Data were based on the total number of offspring obtained.

TABLE 3

Genotyping of Fgf8/Fbln1 double heterozygote mouse cross

Mouse heterozygotes for both Fgf8 and Fbln1 were crossed together, and animals were genotyped at 4 weeks of age. The number of animals observed for the double heterozygote animals was lower than the expected Mendelian ratio as indicated by the boldface number. The χ^2 test statistics test was used to calculate a p value to determine significant deviation from normal expected Mendelian genotypic ratios. Animals with a $(-/-)$ genotype for the Fgf8 allele (boldface symbols) were embryonic lethal and were neither expected to survive nor observed and were not included in the calculation. χ^2 test was significant at $X^2 = 0.010$.

Genotype (Fgf8) (Fbln1)	% expected[a]	% observed	No. expected[a]	No. observed
(**+**/**+**) (+/+)	12%	15%	21	28
(**+**/**+**) (+/−)	22%	26%	43	50
(**+**/**−**) (+/+)	22%	26%	43	51
(**+**/**−**) (+/−)	44%	**33%**	86	64
Total	100%	100%	193	193

[a] Data were based on the total number of offspring obtained.

TABLE 4

Genotyping of Fgf8/Fbln1 double heterozygote mice cross

Mouse heterozygotes for both Fgf8 and Fbln1 were crossed together, and animals were genotyped at 14.5 dpc. The number of animals and the expected Mendelian ratio for the double heterozygote animals was the same (32 *versus* 33). The only genotype that showed deviation from expected Mendelian ratio was the Fgf8 heterozygote and Fbln1 null (boldface number). The χ^2 statistics test was used to calculate a p value to determine significant deviation from normal expected Mendelian genotypic ratios. Animals with a $(-/-)$ genotype for the Fgf8 allele are embryonic lethal and were neither expected to survive nor observed and were not included in the calculation. χ^2 test was significant at $X^2 = 0.022$.

Genotype (Fgf8) (Fbln1)	% expected	% observed	No. expected	No. observed
(**+**/**+**) (+/+)	8%	14%	5	9
(**+**/**+**) (+/−)	17%	16%	11	10
(**+**/**+**) (−/−)	8%	11%	5	7
(**+**/**−**) (+/+)	17%	21%	11	13
(+/−) (+/−)	33%	32%	21	20
(+/−) (−/−)	17%	**6%**	11	4
Total	100%	100%	63	63

TABLE 5

Genotyping of Fgf8/Fbln1 double heterozygote mouse cross

Mouse heterozygotes for both Fgf8 and Fbln1 were crossed together, and animals were genotyped at 16.5 dpc. The number of animals observed for the double heterozygote animals was lower than the expected Mendelian ratio as indicated by the boldface number. The χ^2 statistics test was used to calculate a p value to determine significant deviation from normal expected Mendelian genotypic ratios. Animals with a $(-/-)$ genotype for the Fgf8 allele are embryonic lethal and were neither expected to survive nor observed and were not included in the calculation. χ^2 test was significant at $X^2 = 0.039$.

Genotype (Fgf8) (Fbln1)	% expected	% observed	No. expected	No. observed
(**+**/**+**) (+/+)	8%	14%	4	7
(**+**/**+**) (+/−)	17%	20%	8	10
(**+**/**+**) (−/−)	8%	12%	4	6
(**+**/**−**) (+/+)	17%	24%	8	12
(+/−) (+/−)	33%	**20%**	16	10
(+/−) (−/−)	17%	8%	8	4
Total	100%	100%	49	49

tem and leads to defective NCC migration from rhombomeres 6 and 7 resulting in abnormal formation of cranial nerves IX and X (26). In fact, $\alpha5\beta1$ FN interactions have been shown to be crucial for maintenance of mesodermal derivatives during post-gastrulation stages and also for the survival of some NCCs (20). Integrin $\alpha5\beta1$ null embryos have cranial neural crest and endodermal cell death, which were shown to occur along their migration pathways (27). Although FN and FGF8 interaction has never been reported, binding of FN to its receptor $\alpha5\beta1$ has been shown to regulate FGF8 signaling in the pharyngeal arch region (27). Because FBLN1 is a major binding partner of FN (28), it is possible that the FBLN1 effects on NCC migration might be regulated through partnership with FN along the migration paths from the hindbrain.

The mechanism by which FBLN1 affects FGF8 functions/signaling needs further investigation. It is plausible to suggest that FBLN1 sequesters FGF8 in the extracellular matrix and prevents it from binding to its receptor as demonstrated by our immunohistochemistry and signaling experiments. Moreover, preventing its enzymatic degradation helps in maintaining FGF8 activity in tissues that would be later released by a yet unknown mechanism. We can only speculate at this moment about the significance of FGF8 sequestration by FBLN1 because we have not identified the presence of another receptor system for this complex. It is possible that fibulin-1 might hand off the FGF8 molecule stored extracellularly to the FGF receptor after a certain signal is initiated in a manner similar to extracellular proteoglycans storage of FGF2 and its release to the FGF receptor by the activity of certain heparinases (29).

We were unable to find any report indicating that FBLN1 binds to the promoter region of any gene, thus affecting its expression. However, *FBLN1* promoter sequences have been characterized and found to contain Sp1- and Sp3-binding sites, which are active in regulating the expression of FBLN1 (30). In contrast, the regulation of the *FGF8* gene is more complicated. Marinić *et al.* (31) identified the enhancers of *FGF8* gene expression in mammalian embryogenesis as elements interspersed within unrelated genes (220-kb region) upstream of the start site that act only on FGF8 according to their position within this region and not their sequence.

We speculate that FBLN1 might be acting at an upstream effector of the FGF8 signaling pathway such as sonic hedgehog. We have evidence that FBLN1 binds to the sonic hedgehog with high affinity and that FBLN1 affects sonic hedgehog expression.[6] We hypothesize that FBLN1 might be affecting FGF8 at the level of sonic hedgehog as well as a direct interaction to maintain its presence and availability for NCC survival. Although there is a high degree of redundancy in FGF protein family signaling, it appears that the interaction of FBLN1 and FGF8 is not compensated by other members of the FGF family (mainly FGF3 (32) and FGF24 (33)) to rescue the double heterozygote embryos. Moreover, the interaction of FBLN1

[6] W. O. Twal, unpublished data.

and FGF8 might be unique because the FBLN1/FGF2 interaction did not have any effects on cell signaling.

Recently, two reports in the literature have implicated proteoglycans in the proper development of the heart and outflow tract. The first report described the development of the DeGeorge syndrome-like phenotype in mice deficient in the heparan sulfate-generating enzyme GlcNAc *N*-deacetylase/GlcN *N*-sulfotransferase 1 (NDST1) (34) similar to those exhibited by FGF8 (16) and Fbln-1 (7) null mice. In the second report mutations in the glycosyltranferase enzyme Ext1 result in outflow tract defects that can be reversed using FGF8 (35). It is interesting to speculate that proteoglycans, FBLN1, which is involved proteoglycan processing (9, 36), and FGF8 all play a cooperative role in the maintenance and guidance of NCC to ensure proper cell migration and population in the second heart field and outflow tract for proper development.

We propose that FBLN1 is required for FGF8-dependent NCC guidance and/or survival in the hindbrain by sustaining FGF8 signaling through protection from enzymatic degradation in the extracellular matrix milieu. Preventing NCC death in the hindbrain by maintaining FGF8 signaling ensures that adequate numbers of NCCs migrate and populate the secondary heart field and pharyngeal arches for proper development.

Experimental Procedures

Cells—P19 cells (37) were kindly provided by Dr. Kyu-Ho Lee (Medical University of South Carolina) and used to test the effects of *FBLN1* (38) on *FGF8* gene expression.

Antibodies—Polyclonal antibody Rb2954 recognizes all FBLN1 variants. Monoclonal antibodies 3A11, which recognizes FBLN1 variants A–D with epitope mapping to the N-terminal anaphylatoxin region, and 5D12, which recognizes FBLN1C variant, were described earlier (38). Anti-pERK1/2 monoclonal antibody (clone 20G11) and anti-ERK2 were purchased from Cell Signaling. Monoclonal and polyclonal antibodies against FGF8 as well as FGF8b protein (carrier-free) were purchased from R&D Systems. Anti-disintegrin and metallopeptidase domain 17/tumor necrosis α-convertase (ADAM17/TACE) monoclonal antibody and the ectodomain protein (52 kDa) were from R&D Systems.

FGF8b Binding to Placental FBLN1 using ELISA Procedure—Human FBLN1, purified from placenta, or FGF8b was coated on a 96-well ELISA plate (Nunc) overnight at 4 °C in Tris-buffered saline (TBS, pH 8.0) buffer. Wells were then rinsed and blocked with 1.5% gelatin for 1.5 h at room temperature and then incubated the first well with 120 nM FGF8b and subsequent wells at 1:3 dilutions for a total of six dilutions in TBS buffer containing 0.1% Tween 20 (TBST). FBLN1 was incubated at a concentration of 100 nM in the first well and 1:3 serial dilutions as described for FGF8b in TBST containing 100 μg/ml heparin. Incubations were performed at 4 °C overnight, and then wells were rinsed three times with TBST and incubated with anti-FGF8 monoclonal antibody at 0.5 μg/ml in TBST containing 0.5% gelatin or monoclonal anti-fibulin-1 antibody (3A11) and secondary horseradish peroxidase (HRP)-conjugated antibody at 0.2 μg/ml for 2 h at room temperature. Color development was done using ultra-3,3,5,5-tetramethylbenzidine reagent (Thermo, Pierce) as per the manufacturer's instructions.

Binding of FGF8b to FBLN1 Using Surface Plasmon Resonance—Reichert SR7000DC instrument was used to demonstrate that FGF8b and FBLN1 bind to each other with high affinity. Monoclonal antibody against FGF8 was immobilized on the surface of planar polyethylene glycol/carboxyl sensor chip using amine coupling chemistry and then FGF8b was passed over and captured by the antibody at room temperature in phosphate-buffered saline (PBS) containing 0.1% Tween 20 (PBST). Then 320 nM FBLN1 was injected over the antibody-captured FGF8b, and binding was recorded using a binding sensorgram. Association (k_a) and dissociation (k_d) affinities as well as the affinity constant K_D were calculated.

Immunoprecipitation of FGF8b Using FBLN1-conjugated Sepharose—Placental FBLN1 was conjugated to cyanogen bromide-activated Sepharose at 1.15 mg/ml gel. Fifty microliters of the FBLN1-conjugated beads were mixed with 500 ng of FGF8b diluted in 5 μl of PBS. Twenty microliters of TBST containing 1 mM $CaCl_2$ was added and incubated overnight at 4 °C with end over end agitation. Tubes were then spun down, and supernatant was removed and mixed with 4× non-reducing sample buffer. The FBLN1-conjugated beads were rinsed three times with TBST, and 40 μl of 2× non-reducing sample buffer was added. Plain CL-4B-Sepharose beads were used as negative controls. Bound and unbound fractions were resolved on 4–12% NUPAGE gel (Novex, Life Technologies, Inc.). Proteins were transferred to polyvinylidene fluoride (PVDF) membrane and blocked with 5% nonfat milk. Proteins were visualized using monoclonal antibody against FGF8 at 0.2 μg/ml, HRP-conjugated secondary antibody at 0.1 μg/ml, and enhanced chemiluminescent (ECL+) reagent (GE Healthcare).

Detection of FGF8 in Purified FBLN1, Recombinant Fibulin-1C, and Recombinant Fibulin-1D Preparations—FBLN1, rFBLN1C, or rFBLN1D (2.73 μg/well) (39) was electrophoresed onto 4–12% NUPAGE gels. FGF8b was loaded at 50 ng/lane (positive control). After transfer onto PVDF membrane and blocking with 5% nonfat milk, the blots were incubated overnight at 4 °C with monoclonal antibody against FGF8 at 0.5 μg/ml and secondary anti-mouse horseradish peroxidase-conjugated IgG at 0.4 μg/ml. ECL+ reagent was used for detection. Blots were re-probed after stripping with 100 mM glycine buffer, pH 2.3, with either polyclonal antibody against fibulin-1 (Rb2954) or monoclonal antibody against FBLN1 (3A11) at 0.5 μg/ml. Secondary antibody was used at 0.4 μg/ml, and ECL reagent was used for chemiluminescent detection.

Placental FBLN1 Protection of FGF8b from Enzymatic Degradation—In a total volume of 30 μl, 150 ng of FGF8b were incubated 1) alone, 2) with 1.4 μg of FBLN1, 3) with 0.2 μg of ADAM17/TACE, 4) with 1.4 μg of FBLN1 and 0.2 μg of ADAM17/TACE, or 5) with 5 mM EDTA. Incubation was performed at 4 °C and then 10 μl of non-reducing sample buffer was added, and the incubation reaction was run on 4–12% NUPAGE gel and immunoblotted for FGF8 as described above. Membrane was re-blotted with anti-ADAM17/TACE antibody at 0.2 μg/ml and detected using ECL prime chemiluminescent reagent (GE Healthcare).

FGF8b Activation of Phospho-ERK1/2 (pERK1/2) Signaling Molecules—NIH 3T3 cells (1.0×10^6/well, 6-well plate) were cultured for 18 h in serum-containing medium and then switched to serum-free medium containing insulin, transferrin, and sodium selenite (ITS, Corning Glass) for another 30 h. Cells were then treated with 25 ng/ml FGF8b in the presence or absence of 1.5 μg of FBLN1 for 5 min, and the cell layer was then rinsed with cell rinsing buffer (Bio-Rad BioPlex reagent), and cells in each well were extracted with 300 μl of extraction buffer (Bio-Rad BioPlex phosphoprotein extraction reagent) containing enzyme inhibitors according to the manufacturer's protocol. Basic fibroblast growth factor (FGF2, 25 ng/ml) was used as a control protein. Total protein in the cell extract was quantified using Pierce BCA assay (Thermo Scientific), and a total of 30 μg of protein was loaded in each well of a 4–12% NUPAGE gel. Proteins were transferred to PVDF membrane and blocked with 5% nonfat milk and visualized using antibodies against pERK1/2 and ECL+ as mentioned above. The immunoblot was re-probed with anti-total ERK2 as a loading control. A parallel experiment was also conducted to measure the levels of pERK1/2 in the NIH 3T3 cell extracts (5 μg of total protein/well in duplicate) of FGF8b treatment in the presence or absence of rFBLN-1C, rFBLN-1D, or FBLN1 using Luminex-based assay from Bio-Rad as per the manufacturer's protocol.

Real Time qPCR Detection of FGF8 Transcripts in HT1080 Cells Transfected with FBLN1C and FBLN1D Coding Plasmids—TaqMan assay procedure (Roche Applied Science) was used to detect *FGF8* mRNA expression in control (empty vector) and rFBLN1C- and rFBLN1D-transfected HT1080 cells. Briefly, hydrolysis probe 67 (human universal probe library, Roche Applied Science) was used with two primers listed in Table 1 to detect FGF8 message from stably transfected HT1080 cells (39). Total RNA was isolated from cells cultured on FN-coated 6-well plates in serum-free DMEM using the RNeasy plus kit (Qiagen). cDNA was made using iScript cDNA synthesis kit (Bio-Rad) according to the manufacturer's protocol from 1 μg of total RNA. Twenty microliters of qPCR mixture was made according to the manufacturer's instructions using FastStart Universal Probe Master (Rox) containing 250 nM hydrolysis probe and 900 nM of each primer. The cycling parameters using a CFX96 thermo cycler (Bio-Rad) were 95 °C for 10 min, 40 cycles of 95 °C for 15 s, and 60 °C for 60 s. Primers specific for fibulin-1 variants C and D were also used to detect fibulin-1C and -1D transcripts (Table 1). Regular qPCR assay was used to detect *FBLN1C* and *FBLN1D* transcripts as well as the housekeeping genes. Cycling parameters using Bio-Rad's Evagreen assay supermix were 95 °C for 3 min, 40 cycles of 95 °C for 10 s, 60 °C for 30 s, and 72 °C for 30 s with final extension at 72 °C for 7 min. Melting curve was run from 55 to 95 °C every 0.5 °C to verify the presence of a single amplicon in the reaction mixture. Expression data were analyzed using the PCR miner method (40).

Inhibition of FBLN1 in P19 Mouse Embryonal Teratocarcinoma Cells Using siRNA—Transfection of P19.CL6 cells was performed using nucleofection according to the manufacturer's recommended procedure (Amaxa, Transfection Kit V, program C-020). Briefly, 2.0×10^6 cells were transfected with 30 pmol of either FBLN1 or control Stealth RNAi siRNA (Life Technologies, Inc.). Cells were plated at 1.25×10^5 cells/well of a 6-well tissue culture plate and allowed to attach in complete medium (α-minimal essential medium supplemented with 10% fetal bovine serum). At 0–5 days after electroporation, wells were extracted, and total RNA was prepared using the RNeasy kit (Qiagen). Quality of the total RNA was assessed using an Agilent system. The qPCR experiments for detecting *FGF8, FBLN1C, FBLN1D,* and the housekeeping genes B-actin, *HPRT1,* and *YWHAZ* were conducted using Bio-Rad's Evagreen qPCR master mix in a 25-μl total reaction volume using an iCycler qPCR machine (Bio-Rad). Cycling parameters were described above.

Immunofluorescence Detection of Fgf8 and Fbln1—Immunodetection of both Fgf8 and Fbln1 proteins was performed on histological sections of mouse hearts at 10.5 dpc. Embryos were harvested at 10.5 dpc and fixed in 4% paraformaldehyde and embedded in paraffin. Sections were cut, rehydrated, and then treated for 1 min at high temperature with citrate-based antigen retrieval solution (Vector Laboratories). Sections were then blocked with 1% bovine serum albumin and incubated overnight with monoclonal antibody against FGF8 at 10 μg/ml and with polyclonal anti-FBLN1 IgG (Rb1323) at 15 μg/ml at 4 °C. After three rinses with PBST, the sections were incubated with Alexa 633-conjugated anti-mouse IgG and FITC-conjugated anti-rabbit IgG (Jackson ImmunoResearch) for 2 h at room temperature. Sections were rinsed three times in TBST and mounted in mounting media containing propidium iodide. Control sections were incubated with purified IgG instead of the primary antibodies. Sections were analyzed using a Leica TCS SP5 Confocal AOBS microscope system (Leica Microsystems Inc., Exton, PA). Images were taken at the same laser power and gain settings to compare with IgG control sections.

Generation of Fgf8 Mutant—The Fgf8-deficient mouse strain used in this work was generated from an *Fgf8*-deficient mouse strain containing a non-hypomorphic conditional allele and maintained in 50% each of C57Bl6 and SV129 strain background. This mouse strain has been previously described and was generously provided to us by Dr. Anne Moon (19). The *Fgf8* conditional allele contains a *loxP* site 5′ to exon 4, and a flippase recognition target (*Frt*)-flanked Neo and *loxP* site in the 3′-untranslated region. The *loxP* sites were positioned within the *Fgf8* allele such that Cre recombinase, when expressed, deletes exons 4 and 5, creating a nonfunctional allele. A total of 38 blastocysts were received and implanted in surrogate females at the Gene Targeting and Knock-out Mouse Facility, Medical University of South Carolina. Upon reaching reproductive maturity, a female mutant mouse containing the *Fgf8* conditional allele was mated with a male C57BL/6-Tg(Zp3-Cre)-93Knw/J mouse obtained from The Jackson Laboratory (strain JR 003651). This is a transgenic mouse in which Cre recombinase expression is controlled by the promotor sequence from the mouse zona pellucida 3 (Zp3) gene and directs expression in the growing oocyte prior to completion of the first meiotic division. Initial genotypic analyses examined offspring from matings between *Fgf8* heterozygous mice ($Fgf8^{+/-}$) and *Fbln1* heterozygous mice ($Fbln1^{+/-}$). The χ^2 test statistic was used to calculate a p value by comparing the calculated values to the χ^2 distribution to determine significant delineation from

normal Mendelian genotypic ratios. Subsequent genotypic analyses examined offspring from matings between compound heterozygous mice for both *Fgf8* and *FBLN1* ($Fgf8^{+/-}$ $Fbln1^{+/-}$).

Genotyping—The genotypes of offspring were determined from tail clip genomic DNA by PCR. To detect the wild-type *Fbln1* allele, PCR was performed using *Fbln1* genotyping primers (Table 1). To detect the mutated *Fbln1* allele, the *Fbln1* genotyping reverse primer was used with a CD4 primer (Table 1). Cycling parameters for PCR were as follows: 30 cycles of 95 °C for 30 s, 60 °C for 30 s, and 72 °C for 1 min. The expected size for the amplicon produced from the wild-type *Fbln1* allele is 308 bp. The expected size for the amplicon produced from mutant *Fbln1* allele is 414 bp. To detect the wild-type and non-hypomorphic conditional *Fgf8* allele, PCR was performed using *Fgf8* wild-type allele primers. The expected size for the amplicon produced from the wild-type allele is 214 bp. The expected size for the amplicon produced from the non-hypomorphic conditional *Fgf8* allele is 260 bp. To detect the *Fgf8* recombined null allele, *Fgf8* recombinant mutant allele primers (Table 1) were used in the amplification mixture. The expected size for the amplicon produced from the *Fgf8* recombined null allele is 300 bp. The PCR cycling parameters for detection of all *Fgf8* alleles were 30 cycles of 95 °C for 30 s, 55 °C for 30 s, and 72 °C for 1 min.

Author Contributions—W. O. T. conducted and analyzed all the experiments presented in Figs. 1–6 and wrote the manuscript. V. M. F. conducted the experiments that generated the double knock-out mouse and did the genotyping of mice. C. B. K. conducted the immunofluorescence experiments and data analysis. M. M. designed and constructed plasmids to express recombinant FGF8b and critically revised the manuscript.

Acknowledgments—This study was conceived and supervised by Dr. W. S. Argraves in his laboratory. Dr. Argraves passed away in May 2014. We thank Dr. Derek Beahm (Reichert Analytical Instruments) for conducting the SPR experiments and Drs. Samar M. Hammad and Bryan P. Toole (Medical University of South Carolina) for helpful discussions. We also thank Loren E. Dupuis (Medical University of South Carolina) for immunofluorescence expertise.

References

1. Argraves, W. S., Greene, L. M., Cooley, M. A., and Gallagher, W. M. (2003) Fibulins: physiological and disease perspectives. *EMBO Rep.* **4,** 1127–1131
2. Cooley, M. A., and Argraves, W. S. (2011) in *Biology of Extracellular Matrix: The Extracellular Matrix: An Overview* (Mecham, R. P., ed) pp. 337–367, Springer, Berlin
3. Balbona, K., Tran, H., Godyna, S., Ingham, K. C., Strickland, D. K., and Argraves, W. S. (1992) Fibulin binds to itself and to the carboxyl-terminal heparin-binding region of fibronectin. *J. Biol. Chem.* **267,** 20120–20125
4. Twal, W. O., Czirok, A., Hegedus, B., Knaak, C., Chintalapudi, M. R., Okagawa H., Sugi Y., and Argraves W. S. (2001) Fibulin-1 suppression of fibronectin-regulated cell adhesion and motility. *J. Cell Sci.* **114,** 4587–4598
5. Zhang, H. Y., Kluge, M., Timpl, R., Chu, M. L., and Ekblom, P. (1993) The extracellular matrix glycoproteins BM-90 and tenascin are expressed in the mesenchyme at sites of endothelial-mesenchymal conversion in the embryonic mouse heart. *Differentiation* **52,** 211–220
6. Spence, S. G., Argraves, W. S., Walters, L., Hungerford, J. E., and Little, C. D. (1992) Fibulin is localized at sites of epithelial-mesenchymal transitions in the early avian embryo. *Dev. Biol.* **151,** 473–484
7. Cooley, M. A., Kern, C. B., Fresco, V. M., Wessels, A., Thompson, R. P., McQuinn, T. C., Twal, W. O., Mjaatvedt C. H., Drake, C. J., and Argraves, W. S. (2008) Fibulin-1 is required for morphogenesis of neural crest-derived structures. *Dev. Biol.* **319,** 336–345
8. Kubota, Y., Kuroki, R., and Nishiwaki K. (2004) A fibulin-1 homolog interacts with an ADAM protease that controls cell migration in *C. elegans*. *Curr. Biol.* **14,** 2011–2018
9. Kern, C. B., Twal, W. O., Mjaatvedt, C. H., Fairey, S. E., Toole, B. P., Iruela-Arispe, M. L., and Argraves, W. S., (2006) Proteolytic cleavage of versican during cardiac cushion morphogenesis. *Dev. Dyn.* **235,** 2238–2247
10. Lorenzi, M. V., Long, J. E., Miki, T., and Aaronson, S. A. (1995) Expression cloning, developmental expression and chromosomal localization of fibroblast growth factor-8. *Oncogene* **10,** 2051–2055
11. Ghosh, A. K., Shankar, D. B., Shackleford G. M., Wu, K., T'Ang, A., Miller, G. J., Zheng, J., and Roy-Burman, P. (1996) Molecular cloning and characterization of human FGF8 alternative messenger RNA forms. *Cell Growth Differ.* **7,** 1425–1434
12. Olsen, S. K., Li, J. Y., Bromleigh, C., Eliseenkova, A. V., Ibrahimi, O. A., Lao, Z., Zhang, F., Linhardt, R. J., Joyner, A. L., and Mohammadi, M. (2006) Structural basis by which alternative splicing modulates the organizer activity of FGF8 in the brain. *Genes Dev.* **20,** 185–198
13. Wilson, D. I., Burn, J., Scambler, P., and Goodship, J. (1993) DiGeorge syndrome: part of CATCH 22. *J. Med. Genet.* **30,** 852–856
14. Vitelli, F., Taddei, I., Morishima, M., Meyers, E. N., Lindsay, E. A., and Baldini, A. (2002) A genetic link between Tbx1 and fibroblast growth factor signaling. *Development* **129,** 4605–4611
15. Moon, A. M., Guris, D. L., Seo, J. H., Li, L., Hammond, J., Talbot, A., and Imamoto, A. (2006) Crkl deficiency disrupts FGF8 signaling in a mouse model of 22q11 deletion syndromes. *Dev. Cell* **10,** 71–80
16. Frank, D. U., Fotheringham, L. K., Brewer, J. A., Muglia, L. J., Tristani-Firouzi, M., Capecchi, M. R., and Moon, A. M. (2002) An FGF8 mouse mutant phenocopies human 22q11 deletion syndrome. *Development* **129,** 4591–4603
17. Bockman, D. E., Redmond, M. E., and Kirby, M. L. (1989) Alteration of early vascular development after ablation of cranial neural crest. *Anat. Rec.* **225,** 209–217
18. Ilagan, R., Abu-Issa, R., Brown, D., Yang, Y. P., Jiao, K., Schwartz, R. J., Klingensmith, J., and Meyers, E. N. (2006) FGF8 is required for anterior heart field development. *Development* **133,** 2435–2445
19. Park, E. J., Ogden, L. A., Talbot, A., Evans, S., Cai, C. L., Black, B. L., Frank, D. U., and Moon, A. M. (2006) Required tissue specific roles for FGF8 in outflow tract formation and remodeling. *Development* **133,** 2419–2433
20. Goh, K. L., Yang, J. T., and Hynes, R. O. (1997) Mesodermal defects and cranial neural crest apoptosis in α5 integrin embryos. *Development* **124,** 4309–4319
21. Sato, A., Scholl, A. M., Kuhn, E. N., Kuhn, E. B., Stadt, H. A., Decker, J. R., Pegram, K., Hutson, M. R., and Kirby, M. L. (2011) FGF8 signaling is chemotactic for cardiac neural crest cells. *Dev. Biol.* **354,** 18–30
22. Twal, W. O., Hammad, S. M., Guffy, S. L., and Argraves, W. S. (2015) A novel intracellular fibulin-1D variant binds to the cytoplasmic domain of integrin β1 subunit. *Matrix Biol.* **43,** 97–108
23. Farley, A. M., Morris, L. X., Vroegindeweij, E., Depreter, M. L., Vaidya, H., Stenhouse, F. H., Tomlinson, S. R., Anderson, R. A., Cupedo, T., Cornelissen, J. J., and Blackburn, C. C. (2013) Dynamics of thymus organogenesis and colonization in early human development. *Development* **140,** 2015–2026
24. Greenberg, J. H., Seppä, S., Seppä, H., and Tyl Hewitt, A. (1981) Role of collagen and fibronectin in neural crest cell adhesion and migration. *Dev. Biol.* **87,** 259–266
25. Rovasio, R. A., Delouvee, A., Yamada, K. M., Timpl, R., and Thiery, J. P. (1983) Neural crest cell migration: requirements for exogenous fibronectin and high cell density. *J. Cell Biol.* **96,** 462–473
26. Pietri, T., Eder, O., Breau, M. A., Topilko, P., Blanche, M., Brakebusch, C., Fässler R., Thiery, J.-P., and Dufour, S. (2004) Conditional β1-integrin

gene deletion in neural crest cells causes severe developmental alterations of the peripheral nervous system. *Development* **131,** 3871–3883
27. Mittal, A., Pulina, M., Hou, S. Y., and Astrof, S. (2013) Fibronectin and integrin α5 play requisite roles in cardiac morphogenesis. *Dev. Biol.* **381,** 73–82
28. Tran, H., VanDusen, W. J., and Argraves, W. S. (1997) The self-association and fibronectin-binding sites of fibulin-1 map to calcium-binding epidermal growth factor-like domains. *J. Biol. Chem.* **272,** 22600–22606
29. Bashkin, P., Doctrow, S., Klagsbrun, M., Svahn, C. M., Folkman, J., and Vlodavsky, I. (1989) Basic fibroblast growth factor binds to subendothelial extracellular matrix and is released by heparitinase and heparin-like molecules. *Biochemistry* **28,** 1737–1743
30. Castoldi, M., and Chu, M. L. (2002) Structural and functional characterization of the human and mouse fibulin-1 gene promoters: role of Sp1 and Sp3. *Biochem. J.* **362,** 41–50
31. Marinić, M., Aktas, T., Ruf, S., and Spitz, F. (2013) An integrated holo-enhancer unit defines tissue and gene specificity of the FGF8 regulatory landscape. *Dev. Cell* **24,** 530–542
32. Phillips, B. T., Bolding, K., and Riley, B. B. (2001) Zebrafish fgf3 and fgf8 encode redundant functions required for otic placode induction. *Dev. Biol.* **235,** 351–365
33. Draper, B. W., Stock, D. W., and Kimmel, C. B. (2003) Zebrafish fgf24 functions with fgf8 to promote posterior mesodermal development. *Development* **130,** 4639–4654
34. Pan, Y., Carbe, C., Kupich, S., Pickhinke, U., Ohlig, S., Frye, M., Seelige R., Pallerla, S. R., Moon, A. M., Lawrence, R., Esko, J. D., Zhang, X., and Grobe, K. (2014) Heparan sulfate expression in the neural crest is essential for mouse cardiogenesis. *Matrix Biol.* **35,** 253–265
35. Zhang, R., Cao, P., Yang, Z., Wang, Z., Wu, J. L., Chen, Y., and Pan, Y. (2015) Heparan sulfate biosynthesis enzyme, Ext1, Contributes to outflow tract development of mouse heart via modulation of fgf signaling. *PLoS ONE* **10,** e0136518
36. Lee, N. V., Rodriguez-Manzaneque, J. C., Thai, S. N., Twal, W. O., Luque, A., Lyons, K. M., Argraves, W. S., and Iruela-Arispe, M. L. (2005) Fibulin-1 acts as a cofactor for the matrix metalloprotease ADAMTS-1. *J. Biol. Chem.* **280,** 34796–34804
37. Wang, C., Xia, C., Bian, W., Liu, L., Lin, W., Chen, Y.-G., Ang, S. L., and Jing, N. (2006) Cell aggregation-induced FGF8 elevation is essential for P19 cell neural differentiation. *Mol. Biol. Cell* **17,** 3075–3084
38. Argraves, W. S., Tran, H., Burgess, W. H., and Dickerson, K. (1990) Fibulin is an extracellular matrix and plasma glycoprotein with repeated domain structure. *J. Cell Biol.* **111,** 3155–3164
39. Tran, H., Mattei, M., Godyna, S., and Argraves, W. S. (1997) Human fibulin-1D: molecular cloning, expression and similarity with S71–5 protein, a new member of the fibulin gene family. *Matrix Biol.* **15,** 479–493
40. Zhao, S., and Fernald, R. D. (2005) Comprehensive algorithm for quantitative real time polymerase chain reaction. *J. Comput. Biol.* **12,** 1047–1064